JOC The Journal of Organic Chemistry

Article

Cite This: J. Org. Chem. 2019, 84, 9051−9057

pubs.acs.org/joc

Aryl Carbamates: Mechanisms of Orthosodiations and Snieckus−Fries Rearrangements

Yun Ma, Ryan A. Woltornist, Russell F. Algera, and David B. Collum*

Department of Chemistry and Chemical Biology Baker Laboratory, Cornell University, Ithaca, New York 14853-1301, United States

Supporting Information

ABSTRACT: Aryl carbamates are orthometalated by sodium diisopropylamide (NaDA) in tetrahydrofuran. The resulting arylsodiums undergo Snieckus−Fries rearrangement to give orthoacylated phenols in good yield. The intermediate arylsodiums and resulting orthoacylated phenolates are suggested to be monomeric. The rate-limiting step in the two-step sequence depends on the steric demands of the carbamoyl moiety and the substituents in the meta position of the arene. Rate studies reveal a dominant disolvated-monomer-based orthometalation followed by a di- or trisolvated arylsodium monomer-based rearrangement. Kinetic evidence of a NaDA-catalyzed Snieckus−Fries rearrangement suggests the intermediacy of mixed trimers. Competitive halide eliminations to form benzyne are also discussed.

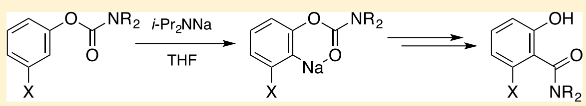

INTRODUCTION

We have an emergent interest in the chemistry of sodium diisopropylamide (NaDA) and the structures and reactivities of the resulting organosodium salts.[1,2] To say that NaDA has received little interest is an understatement. While lithium diisopropylamide (LDA) is used daily, less than two dozen reports of NaDA-mediated metalations appeared over the half-century following the first report in 1960.[3]

NaDA is a much more reactive base than LDA and displays complementary selectivities,[1a] but its adoption has been constrained by its insolubility in hydrocarbons and its propensity toward decomposition in ethers,[1b,3] both exacerbating problems with stock solutions. However, trialkylamines[4] such as *N*,*N*-dimethylethylamine (DMEA) or *N*-methylpyrrolidine have been found to afford stable ≥1.0 M NaDA solutions that can be prepared in minutes from technical-grade reagents on the benchtop without the need for vacuum lines or gloveboxes.[1a,5] We have characterized NaDA in standard donor solvents[1b] and studied the mechanisms of its reactions with alkenes, dienes, arenes, and alkyl halides.[1c−f]

In this paper, we describe NaDA-mediated Snieckus−Fries rearrangements (Scheme 1).[6] The NaDA-mediated metalation step is fast when compared with LDA,[7] and the subsequent rearrangements afford high yields of orthoacylated phenols. Arylsodiums bearing halogen substituents may either rearrange or form benzynes, depending on the nature of the halogen and carbamate substituents.[8]

Scheme 1. Orthometalation and Snieckus−Fries Rearrangements of Aryl Carbamates with Isolated Yields

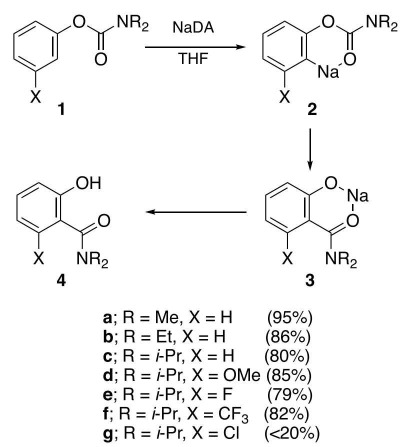

RESULTS AND DISCUSSION

NaDA of adequate purity for synthetic applications can be prepared in situ from technical-grade diisopropylamine and DMEA in minutes. For the structural and rate studies described herein, however, we take the added precaution of using NaDA recrystallized from DMEA−hexane.[1a] NaDA in DMEA or hexane containing ≥3 equiv of tetrahydrofuran (THF) forms exclusively the tetrasolvated dimer **5**;[1b,9] THF/DMEA and THF/hexane may be used interchangeably for generic metalations.[1c−f]

Substantial spectroscopic, kinetic, and computational data are archived in the Supporting Information. Allusions to results that are unaccompanied by specific data are fully documented therein. Density functional theory (DFT) calculations were carried out at the B3LYP/6-31G(d) level[10] with energies from single-point calculations at the M06-2X level of theory.[11] The phrase "computationally viable" alludes to computations affording valid minima and saddle points with a single negative frequency. To homogenize the results, all computations were carried out on the meta fluoro derivatives (the "**e**" series).

Received: April 8, 2019
Published: July 1, 2019

DOI: 10.1021/acs.joc.9b00968
J. Org. Chem. 2019, 84, 9051−9057

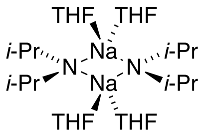

5

Profile of the Reaction Coordinate. Aryl carbamate metalations and subsequent rearrangements were monitored using in situ IR spectroscopy[12] by following the absorbances of the starting carbamates **1a−g** (1720−1734 cm^{-1}), arylsodiums **2b−g** (1680−1697 cm^{-1}), and sodium phenolates **3a−g** (1615−1624 cm^{-1}). (See Figure 1.) By adjusting the aryl substituents (X), carbamate *N*-alkyl groups (R), reaction temperature, and substrate deuteration, we were able to independently monitor the metalation and rearrangement steps (Scheme 2). For example, the rate-limiting metalation of **1a** is followed by rapid rearrangement to **3a**, which precludes the observation of arylsodium **2a**. Switching to the diethylamido moiety (**1b**) has little effect on the rate of metalation, but markedly slows the rearrangement step, causing **2b** to accumulate in a fully established soft (balanced) equilibrium prior to rearrangement. Incorporation of acidifying substituents in the meta position promotes and accelerates the metalations while decelerating the subsequent rearrangements; arylsodiums **2d−g** form quantitatively prior to rearrangement.

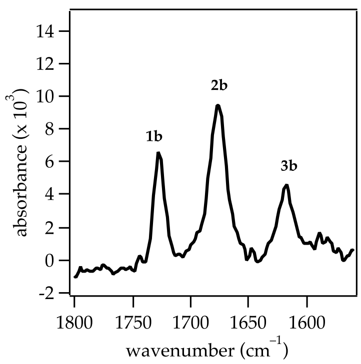

Figure 1. IR spectrum for the metalation and rearrangement of 0.010 M diethylcarbamate **1b** with 0.15 M NaDA in 6.80 M THF/hexane at −50 °C. The spectrum, recorded after 60 s, shows both arylsodium **2b** and phenolate **3b**.

Scheme 2. Intermediate Arylsodiums

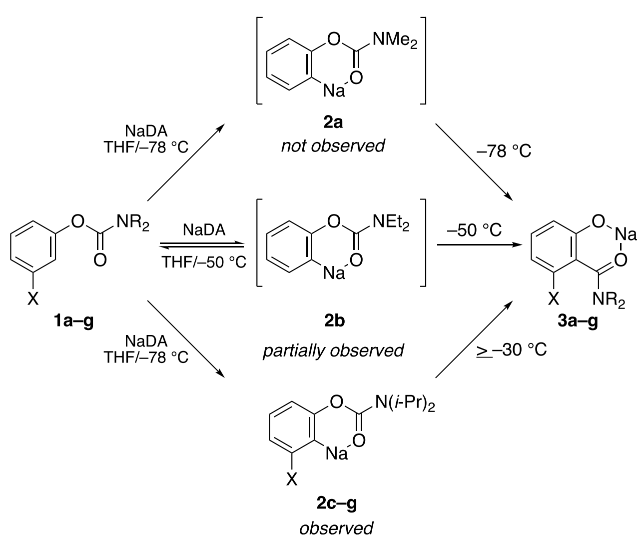

Arylsodium Structures. Unlike aryllithiums in which $^6Li-^{13}C$ coupling provides intimate structural details,[13] less direct methods are needed to characterize the arylsodiums. We favor the method of continuous variations[14] in which binary mixtures of arylsodiums are monitored by ^1H or $^{13}C\{^1H\}$ NMR spectroscopy (eq 1). In principle, the number and symmetries of heteroaggregates should reveal the aggregation state. In practice, no heteroaggregates were observed. While the absence of evidence is not necessarily evidence of absence, it does appear that the ArNa or ArLi stability required for observable metalation with alkali metal amides is also the precondition that precludes aggregation.[13b]

$$(ArNa)_n + (Ar'Na)_n \rightleftharpoons (ArNa)_x(Ar'Na)_y \quad (1)$$

DFT computations on **2e** reveal exothermic serial solvation to afford di-, tri-, and tetrasolvated monomers **6**, **7**, and **8**, respectively (Scheme 3). IR spectroscopy shows a near 50 cm^{-1} shift of the carbonyl to lower energy, suggesting that chelation remains intact. This observation would argue against tetrasolvated **8**, which lacks chelation.[15] Dimerization to generate **9**, which is suggested to form at low THF concentration, is calculated to be endothermic by 8.1 kcal/mol (although such nonisodesmic[16] comparisons should be viewed with great caution).

Scheme 3. Computed Structure of Arylsodium

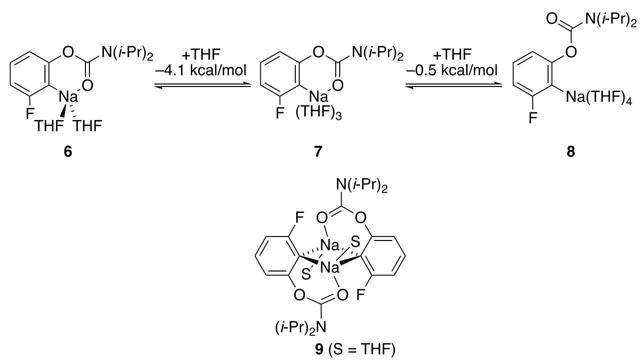

Substrates **1b** and **1c** in which arene and arylsodium coexist at equilibrium, appeared to offer an easy experimental probe of arylsodium solvation benchmarked to tetrasolvated NaDA dimer **5**,[1b] but the results proved confusing. The proportions of ArNa and ArH versus THF concentration (Figure 2) suggest that ArNa monomer **2b** has a lower per-sodium solvation number than NaDA. If one presumes that **2b** remains monomeric at all THF concentrations, these data would imply a monosolvated monomer, which contradicts significant accumulated experience.[1] We submit that the THF dependence (eq 2) arises from dimer formation at low THF concentration. Unfortunately, solubility problems at low THF concentration prevented us from further probing this question.

$$2ArNa(THF)_3 \xrightleftharpoons{-R_2NH,+2THF} ArH + (R_2NNa)_2(THF)_4$$
$$\xrightleftharpoons{-2THF} (ArNa)_2(THF)_2 \quad (2)$$

Sodium Phenolate Structures. Although it is not essential to elucidate the structures of the sodium phenolates

DOI: 10.1021/acs.joc.9b00968
J. Org. Chem. 2019, 84, 9051−9057

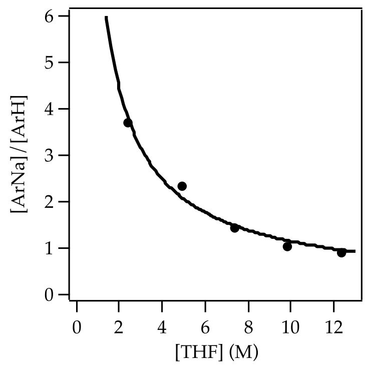

Figure 2. Plot of [ArNa]/[ArH] versus [THF] in hexane for the sodiation of diethylcarbamate **1b** (ArH) to give arylsodium **2b** (ArNa) at equilibrium with 0.10 M NaDA at −50 °C. The curve represents an unweighted overtly simplified least-squares fit to $y = ax^b$ ($a = 8.1 \pm 0.7$, $b = -0.85 \pm 0.07$).

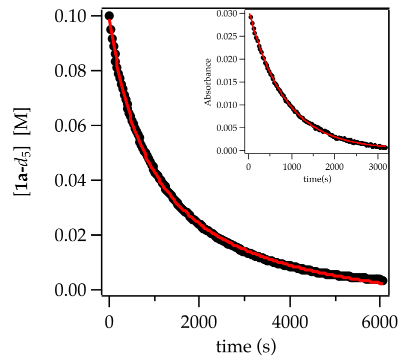

Figure 3. Plot of phenyl-d_5-dimethylcarbamate (**1a**-d_5) concentration versus time for the metalation of 0.10 M **1a**-d_5 with 0.10 M NaDA in 7.5 M THF/hexane at −78 °C. The curve represents an unweighted least-squares fit to the second-order function, $y = a/(1 + bx) + c$ ($a = 0.1128 \pm 0.0002$, $b = -0.00010 \pm 0.00001$, $c = 0.014 \pm 0.001$). Inset: plot of phenyl-d_5-dimethylcarbamate (**1a**-d_5) concentration versus time for the metalation of 0.010 M **1a**-d_5 with 0.10 M NaDA in 7.5 M THF/hexane at −78 °C. $y = -ae^{-bx} + c$ ($a = 0.034 \pm 0.001$, $b = 0.0012 \pm 0.0005$, $c = 0.0028 \pm 0.0001$).

(**3a**−**e**) to understand the Snieckus−Fries rearrangement, we sought to probe these structures owing to their role as intermediates in numerous pharmaceutical transformations en route to aryl ethers.[14,17] There is also a general dearth of details on the solution structures of organosodiums.[2] In short, a binary mixture of phenolates **3e** and **3f** displays no NMR spectroscopic evidence of heteroaggregation, indicating that they are monomeric. DFT computations with **3e** suggest that 5-coordinate trisolvates (eq 3) are more stable.[1c,18−20]

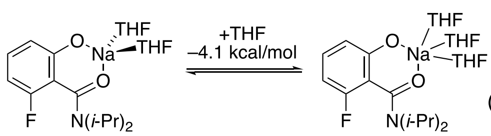

(3)

Kinetics and Mechanism of Orthometalation. Tractable rates observed in the orthometalations of unsubstituted carbamates (assisted by the retarding effects of deuteration) allowed us to probe the mechanism of orthometalation in detail. Metalation of **1a**-d_5 under second-order conditions (1.0 equiv NaDA) follows a decay with no anomalous curvatures that would have attested to autocatalysis or autoinhibition (Figure 3).[21] Metalation of **1a**-d_5 under pseudo-first-order conditions (0.010 M) at −78 °C by 0.10 M NaDA in 7.5 M THF/hexane follows a clean first-order decay (Figure 3, inset). At the completion of the reaction, the baseline was zeroed and a second aliquot of the substrate was added. The two pseudo-first-order rate constants (k_{obsd}) agree within 10%.

Plotting k_{obsd} versus THF concentration (Figure 4) and NaDA concentration (Figure 5) affords zeroth- and half-order dependencies, respectively. The downward drift in the THF dependence is only moderately disconcerting, displaying none of the curvature expected for a true inverse dependence. A routine control experiment[1f] using 2,5-dimethyltetrahydrofuran (Me_2THF) instead of hexane as the cosolvent to maintain the polarity of the medium constant had no effect whatsoever; the downward drift does not appear to derive from secondary-shell (medium) effects. The idealized rate law[22] (eq 4) and assignment of NaDA as tetrasolvated dimer **5**[1b] are consistent with the generic mechanism in eq 5. A comparison of the rates of **1a** and **1a**-d_5 ($k_H/k_D \geq 6$) confirms that proton transfer is rate-limiting.

$$-d[ArH]/dt = k[THF]^0[A_2S_4]^{1/2}[ArH] \quad (4)$$

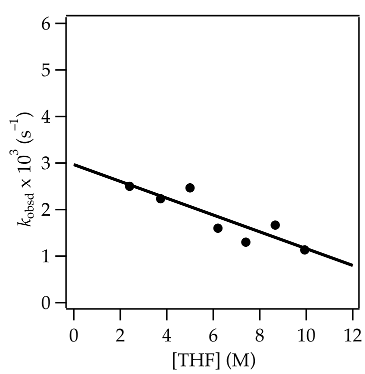

Figure 4. Plot of k_{obsd} versus [THF] in hexane for the orthosodiation of carbamate **1a**-d_5 (0.010 M) by NaDA (0.10 M) at −78 °C. The curve represents an unweighted least-squares fit to $k_{obsd} = k[THF] + k'$ ($k = (-1.8 \pm 0.4) \times 10^{-3}$, $k' = (2.9 \pm 0.3) \times 10^{-3}$).

$$1/2\ A_2(THF)_4 + ArH \rightarrow [A(THF)_2 \cdot ArH]^{\ddagger} \quad (5)$$

The stoichiometry of the transition structure[23] is consistent with a disolvated-monomer-based mechanism. DFT computations (using the **e** series as noted above, Figure 6) confirm that transition structure **10** is computationally viable, with intrinsic reaction coordinate calculations showing **11** as the first-formed product, which appears to rapidly collapse to the carbonyl-complexed form.[24]

Mechanism of Snieckus−Fries Rearrangement. Rearrangement of arylsodium **2a** to phenolate **3a** is an unobservable post-rate-limiting step (Scheme 2). By contrast, **2d** forms rapidly and rearranges slowly. Loss of **2d**, suggested to exist as a trisolvated monomer as described above, follows a first-order decay, manifests a first-order THF dependence with a considerable nonzero intercept (Figure 7), and shows no dependence on the concentration of excess NaDA (Figure 8). The idealized rate law (eq 6) is consistent with the generic mechanism in eqs 7 and 8. DFT computations (staying with the **e** series as noted above, Figure 9) afford a viable trisolvated transition structure **12**, but we could not locate a plausible tetrasolvate corresponding to **13**. Rate data for arylsodium **2f** point to an analogous mechanism.

DOI: 10.1021/acs.joc.9b00968
J. Org. Chem. 2019, 84, 9051−9057

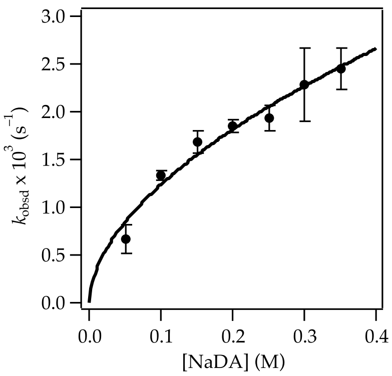

Figure 5. Plot of k_{obsd} versus [NaDA] in 6.2 M THF/hexane for the orthosodiation of carbamate **1a**-d_5 (0.010 M) by NaDA at −78 °C. The curve represents an unweighted least-squares fit to $k_{obsd} = k[\text{NaDA}]^n$ ($k = 0.0044 \pm 0.0004$, $n = 0.55 \pm 0.06$).

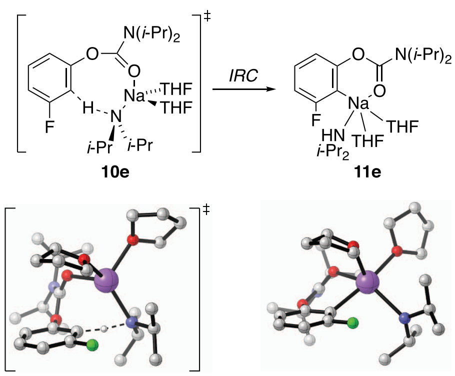

Figure 6. Computed transition structures for orthosodiation.

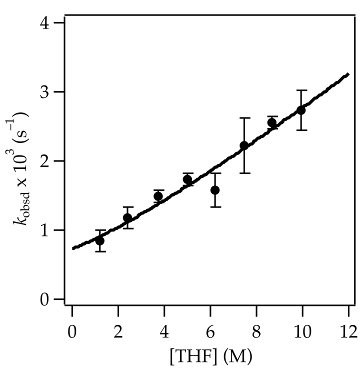

Figure 7. Plot of k_{obsd} versus [THF] in hexane cosolvent for the rearrangement of arylsodium **2d** (0.010 M) by NaDA (0.10 M) at −15 °C. The curve represents an unweighted least-squares fit to $k_{obsd} = k[\text{THF}]^n + k'$ ($k = (0.14 \pm 0.01) \times 10^{-3}$, $k' = (0.7 \pm 0.3) \times 10^{-3}$, $n = 1.17 \pm 0.04$).

$$-\text{d[ArNa]}/\text{d}t = (k + k'[\text{THF}]^1)[\text{ArNa}] \quad (6)$$

$$\underset{\mathbf{2}}{\text{ArNa(THF)}_3} \rightarrow \underset{\mathbf{12}}{[\text{ArNa(THF)}_3]^{\ddagger}} \quad (7)$$

$$\underset{\mathbf{2}}{\text{ArNa(THF)}_3} + \text{THF} \rightarrow \underset{\mathbf{13}}{[\text{ArNa(THF)}_4]^{\ddagger}} \quad (8)$$

NaDA-Catalyzed Snieckus–Fries Rearrangement. Rearrangement of fluoro-substituted arylsodium **2e** displays all of the accoutrements of a disolvated-monomer-based rearrangement. A slight inhibiting influence of THF is well within the norm for a zeroth-order dependence. A dependence on NaDA, however, was unexpected (Figure 10), as was the linearity indicating an apparent first-order rather than half-order dependence. In retrospect, perhaps, this finding should not have come as a surprise, given that a similar LDA catalysis is observed for the Snieckus–Fries rearrangement of the aryllithium analog.[7b]

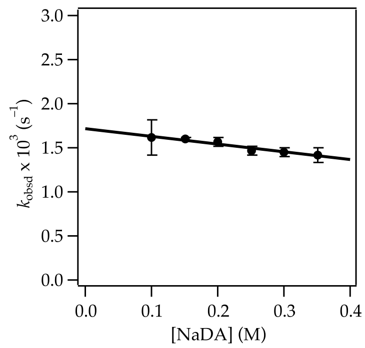

Figure 8. Plot of k_{obsd} versus [NaDA] in 6.2 M THF/hexane for the rearrangement of arylsodium **2d** (0.010 M) at −15 °C. The curve represents an unweighted least-squares fit to $k_{obsd} = k[\text{NaDA}] + k'$ ($k = (-0.9 \pm 0.1) \times 10^{-3}$, $k' = (1.7 \pm 0.1) \times 10^{-3}$).

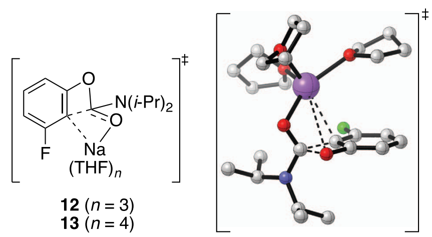

Figure 9. Computed transition structure of the Snieckus–Fries rearrangement.

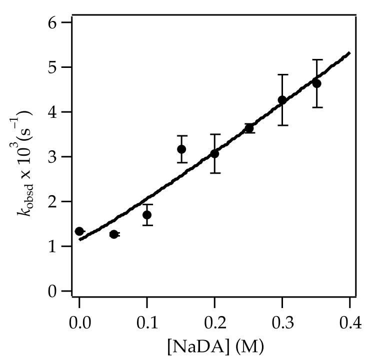

Figure 10. Plot of k_{obsd} versus [NaDA] in 6.2 M THF/hexane for the rearrangement of arylsodium **2e** (0.010 M) at 0 °C. The curve represents an unweighted least-squares fit to $k_{obsd} = k[\text{NaDA}]^n + k'$ ($k = 0.012 \pm 0.004$, $k' = 0.0012 \pm 0.0004$, $n = 1.15 \pm 0.03$).

The rate data for the NaDA-catalyzed rearrangement implicates a mixed-trimer-based transition structure containing two NaDA subunits. We computationally explored the roles of fleeting mixed dimers and mixed trimers to envision the mechanism and offer transition structures **14** and **15** as computationally viable models. A more highly solvated mixed trimer was not computationally viable. The energies were reasonable but are not isodesmic and should not be taken too seriously. Mixed trimer **15**, implicated by the rate studies, does

DOI: 10.1021/acs.joc.9b00968
J. Org. Chem. 2019, 84, 9051−9057

not require that NaDA forfeit the full aggregation energy but, as drawn, requires forfeiting three solvent−sodium contacts from the $ArNa(THF)_3/(R_2NNa)_2(THF)_4$ resting state at an estimated total energetic cost of 5 kcal/mol. (The third THF on the arylsodiums and fourth THF on NaDA are marginally stabilizing.) As a thought experiment, treating mixed dimers and mixed trimers (not shown) as independent ground states, the barriers corresponding to **14** and **15** are of comparable energies.

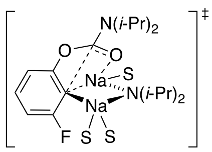

14
(S = THF)

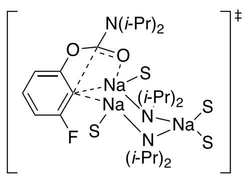

15
(S = THF)

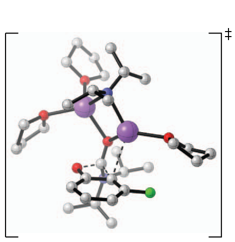

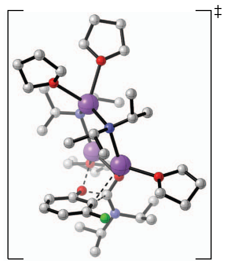

Benzynes. Arylsodiums and aryllithiums bearing halogen substituents may be susceptible to benzyne formation. Thus, while the rearrangement of fluorinated arylsodium **2e** at 0 °C affords phenol **4e** in 79% isolated yield with no observable benzyne-derived products, the rearrangement of the lithium analog of **2e**, generated using LDA, leads to low yields of **4e** along with **17**, **18**, and other debris consistent with benzyne **16**. Reaction of chlorinated arylsodium **2g** at −35 °C affords a low yield of phenol **4g** (<20%) along with benzyne-derived byproducts (Scheme 4).[25]

Scheme 4. Benzyne Formation

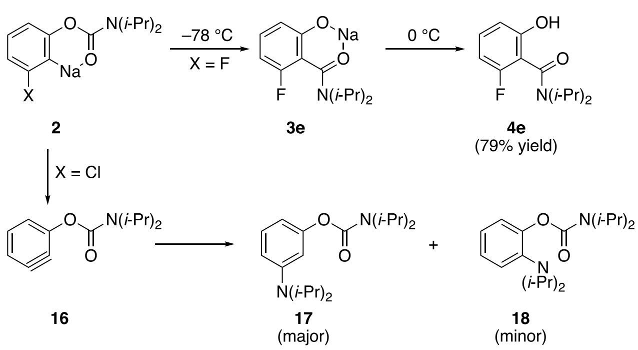

The divergent chemoselectivities of the meta fluoro and chloro derivatives mimic the analogous lithium species. In aryllithiums, LiCl elimination is promoted by high solvent concentration and affiliated lack of a strong Li−Cl contact, whereas LiF elimination is favored by low solvent concentration, which promotes a Li−F contact.[26] Based on the propensity of **2e** to undergo rearrangement in lieu of elimination, we infer that the F−Na interaction is weak.

■ SUMMARY AND CONCLUSIONS

Synthetic chemists have exploited the Snieckus−Fries rearrangement as a means to achieve phenol ortho-functionalization. The internal trapping mechanism also has a probative mechanistic value. The overall reaction coordinate for the tandem orthometalation and subsequent Snieckus−Fries rearrangement is summarized in Scheme 5. Observable intermediates **2** and **3** appear to be di- or trisolvated monomers, as supported by DFT computations. Rate studies implicate the disolvated-monomer-based transition structure **10** for the metalation and the tri- and possibly tetrasolvated-monomer-based transition structures **12** and **13** for the rearrangement. Evidence of a NaDA-catalyzed rearrangement aligns with results from the corresponding lithium-based Snieckus−Fries rearrangement.

Scheme 5. Summary of Structure and Mechanism

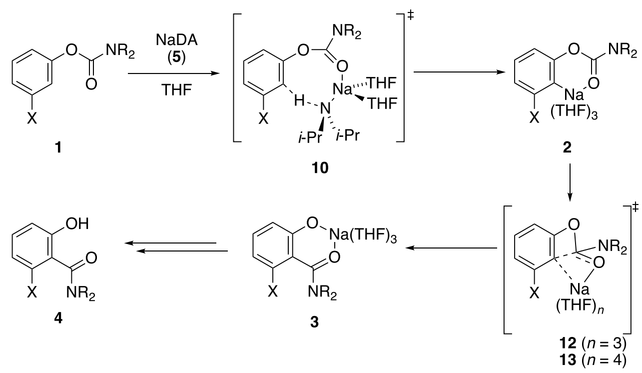

The overarching message is that the sodium analog of the Snieckus−Fries rearrangements works quite well. The orthometalations and rearrangements are markedly faster than their lithium analogs. As we explore the structure−reactivity−selectivity relationships in organosodium chemistry, we are pleased by how well the chemistry works and by the high solubilities of the sodium salts. Although we did detect aggregation effects of consequence, the generally lower frequency of occurrence in organosodium chemistry when compared to that in organolithium chemistry is refreshing and may render organosodium chemistry more predictable in the long run.

■ EXPERIMENTAL SECTION

Reagents and Solvents. THF and hexane were distilled from blue or purple solutions containing sodium benzophenone ketyl. NaDA was prepared and isolated, although control experiments confirm that in situ-generated NaDA/DMEA/THF is indistinguishable. Air- and moisture-sensitive materials were manipulated under argon or nitrogen using standard glovebox, vacuum line, and syringe techniques. Aryl carbamates **1a**−**g** were prepared by literature procedures.[6]

IR Spectroscopic Analyses. IR spectra were recorded using an in situ IR spectrometer fitted with a 30 bounce, silicon-tipped probe. The spectra were acquired in 16 scans at a gain of 1 and a resolution of 4 cm^{-1}. A representative reaction was carried out as follows: the IR probe was inserted through a nylon adapter and O-ring seal into an oven-dried, cylindrical flask fitted with a magnetic stir bar and a T-joint. The T-joint was capped by a septum for injections and a nitrogen line. After evacuation under full vacuum, heating, and flushing with nitrogen, the flask was charged with NaDA (64 mg, 0.10 mmol) in THF (5.0 mL) and cooled in a dry ice−acetone bath prepared with fresh acetone. After recording a background spectrum,

DOI: 10.1021/acs.joc.9b00968
J. Org. Chem. 2019, 84, 9051−9057

we added aryl carbamate **1** (0.010 mmol) with stirring. For the most rapid reactions, IR spectra were recorded every 15 s with monitoring of the absorbance at 1730 cm^{-1} over the course of the reaction.

NMR Spectroscopic Analyses. NMR samples for reaction monitoring and structure determination were routinely prepared using stock solutions of NaDA in THF/hexane mixtures maintained at −80 °C and flame-sealed under partial vacuum. Standard ^{1}H and $^{13}C\{^{1}H\}$ NMR spectra were recorded on a 500 MHz spectrometer at 500 and 125.79 MHz, respectively. The ^{1}H and ^{13}C resonances were referenced to the CH_2O resonance (3.58 ppm) and CH_2O resonance (67.57 ppm) of THF at −80 °C, respectively.

DFT Computations. DFT calculations were carried out at the B3LYP/6-31G(d) level with single-point calculations at the M06-2X level of theory.[10,11] Transition structures each had a single negative frequency.

*2-Fluoro-6-hydroxy-N,N-diisopropylbenzamide (**4e**).* 3-Fluorophenyl diisopropylcarbamate (**1c**, 479 mg, 2.0 mmol) in 5.0 mL of THF was added dropwise over 10 min to a solution of NaDA (2.2 mmol, 271.0 mg) in THF (10.0 mL) at −78 °C under N_2. The resulting solution was warmed to 0 °C, stirred for 2 h, and quenched with saturated aqueous ammonium chloride (8.0 mL). The THF was removed under reduced pressure, and the aqueous residue was extracted with dichloromethane (4 × 10 mL). The combined organic extracts were dried ($MgSO_4$), filtered, and concentrated under reduced pressure to afford the crude product, which was purified using flash column chromatography (8:1 CH_2Cl_2/EtOAc) to give **4e** (79%) as white needles. ^{1}H NMR (500 MHz, $CDCl_3$). δ 8.28 (1H, s), 7.15 (1H, dt, J = 8.3, 6.6 Hz), 6.75 (1H, dt, J = 8.3, 0.8 Hz), 6.58 (1H, ddd, J = 9.3, 8.3, 1.0 Hz), 3.70 (1H, s, br), 1.35 (12H, s, br), $^{13}C\{^{1}H\}$ NMR (125.8 MHz, $CDCl_3$). δ 168.5, 158.5 (d, J_{C-F} = 246.4 Hz), 157.0 (d, J_{C-F} = 6.4 Hz), 132.6 (d, J_{C-F} = 10.6 Hz), 112.0 (d, J_{C-F} = 6.4 Hz), 106.8 (d, J_{C-F} = 22.5 Hz), 20.7. (The isopropyl methinyl carbon is missing owing to a conformational coalescence.) ^{19}F NMR (470.33 MHz, $CDCl_3$) δ −113.8. HRMS (ESI-TOF) m/z $[M + H]^+$ calcd for $C_{12}H_{18}FNO_2$ 240.1399; found 240.1390.

■ ASSOCIATED CONTENT

Supporting Information

The Supporting Information is available free of charge on the ACS Publications website at DOI: 10.1021/acs.joc.9b00968.

^{1}H, $^{13}C\{^{1}H\}$, and ^{19}F NMR spectra; IR spectrum of the metalation rearrangement; plot of absorbance versus time depicting the rearrangement of **2b** from an equilibrium mixture of **1b** and **2b** generated with NaDA; and geometric coordinates and thermally corrected M06-2X energies (PDF)

■ AUTHOR INFORMATION

Corresponding Author

*E-mail: dbc6@cornell.edu.

ORCID

David B. Collum: 0000-0001-6065-1655

Notes

The authors declare no competing financial interest.

■ ACKNOWLEDGMENTS

The authors thank the National Institutes of Health (GM131713) for support.

■ REFERENCES

(1) (a) Ma, Y.; Algera, R. F.; Collum, D. B. Sodium Diisopropylamide in *N,N*-Dimethylethylamine: Reactivity, Selectivity, and Synthetic Utility. *J. Org. Chem.* **2016**, *81*, 11312. (b) Algera, R. F.; Ma, Y.; Collum, D. B. Sodium Diisopropylamide: Aggregation, Solvation, and Stability. *J. Am. Chem. Soc.* **2017**, *139*, 7921. (c) Algera, R. F.; Ma, Y.; Collum, D. B. Sodium Diisopropylamide in Tetrahydrofuran: Selectivities, Rates, and Mechanisms of Alkene Isomerizations and Diene Metalations. *J. Am. Chem. Soc.* **2017**, *139*, 11544. (d) Algera, R. F.; Ma, Y.; Collum, D. B. Sodium Diisopropylamide in Tetrahydrofuran: Selectivities, Rates, and Mechanisms of Arene Metalations. *J. Am. Chem. Soc.* **2017**, *139*, 15197. (e) Zhang, Z.; Collum, D. B. Structures and Reactivities of Sodiated Evans Enolates: Role of Solvation and Mixed Aggregation on the Stereochemistry and Mechanism of Alkylations. *J. Am. Chem. Soc.* **2019**, *141*, 388. (f) Ma, Y.; Algera, R. F.; Woltornist, R. A.; Collum, D. B. Sodium Diisopropylamide-Mediated Dehydrohalogenations: Influence of Primary- and Secondary-Shell Solvation. *J. Org. Chem.* **2019**, submitted.

(2) (a) Mulvey, R. E.; Robertson, S. D. Synthetically Important Alkali-Metal Utility Amides: Lithium, Sodium, and Potassium Hexamethyldisilazides, Diisopropylamides, and Tetramethylpiperidides. *Angew. Chem., Int. Ed.* **2013**, *52*, 11470. (b) Watson, B. T.; Lebel, H. Sodium Hexamethyldisilazide. In *e-EROS Encyclopedia of Reagents for Organic Synthesis*; John Wiley & Sons: New York, 2005; pp 1−10. (c) Seyferth, D. Alkyl and Aryl Derivatives of the Alkali Metals: Useful Synthetic Reagents as Strong Bases and Potent Nucleophiles. 1. Conversion of Organic Halides to Organoalkali-Metal Compounds. *Organometallics* **2006**, *25*, 2. (d) Seyferth, D. Alkyl and Aryl Derivatives of the Alkali Metals: Strong Bases and Reactive Nucleophiles. 2. Wilhelm Schlenk's Organoalkali-Metal Chemistry. The Metal Displacement and the Transmetalation Reactions. Metalation of Weakly Acidic Hydrocarbons. Superbases. *Organometallics* **2009**, *28*, 2. (e) Benkeser, R. A.; Foster, D. J.; Sauve, D. M.; Nobis, J. F. Metalations With Organosodium Compounds. *Chem. Rev.* **1957**, *57*, 867.

(3) (a) Raynolds, S.; Levine, R. The Synthesis of Nitrogen-containing Ketones. VIII. The Acylation of 3-Picoline, 4-Picoline and Certain of their Derivatives. *J. Am. Chem. Soc.* **1960**, *82*, 472. (b) For a bibliography of NaDA-mediated reactions see reference 1b.

(4) For leading references to trialkylamine-solvated lithium amides, see: Godenschwager, P. F.; Collum, D. B. Lithium Hexamethyldisilazide-Mediated Enolizations: Influence of Triethylamine on E/Z Selectivities and Enolate Reactivities. *J. Am. Chem. Soc.* **2008**, *130*, 8726.

(5) The preparation of NaDA in reference 1a is a modified procedure reported previously: Barr, D.; Dawson, A. J.; Wakefield, B. J. A Simple, High-Yielding Preparation of Sodium Diisopropylamide and Other Sodium Dialkylamides. *J. Chem. Soc., Chem. Commun.* **1992**, *2*, 204.

(6) Jalil Miah, M. A.; Sibi, M. P.; Chattopadhyay, S.; Familoni, O. B.; Snieckus, V. Directed ortho-Metalation of *O*-Aryl *N,N*-Dialkylcarbamates: Methodology, Anionic *ortho*-Fries Rearrangement, and Lateral Metalation. *Eur. J. Org. Chem.* **2018**, *2018*, 440.

(7) (a) Singh, K. J.; Collum, D. B. Lithium Diisopropylamide-Mediated Ortholithiation and Anionic Fries Rearrangement of Aryl Carbamates: Role of Aggregates and Mixed Aggregates. *J. Am. Chem. Soc.* **2006**, *128*, 13753. (b) Riggs, J. C.; Singh, K. J.; Ma, Y.; Collum, D. B. Anionic Snieckus-Fries Rearrangement: Solvent Effects and Role of Mixed Aggregates. *J. Am. Chem. Soc.* **2008**, *130*, 13709.

(8) (a) Roy, T.; Biju, A. T. Recent Advances in Molecular Rearrangements Involving Aryne Intermediates. *Chem. Commun.* **2018**, *54*, 2580. (b) Yoshida, S.; Hosoya, T. The Renaissance and Bright Future of Synthetic Aryne Chemistry. *Chem. Lett.* **2015**, *44*, 1450.

(9) Andrews, P. C.; Barnett, N. D. R.; Mulvey, R. E.; Clegg, W.; O'Neil, P. A.; Barr, D.; Cowton, L.; Dawson, A. J.; Wakefield, B. J. X-ray Crystallographic Studies and Comparative Reactivity Studies of a Sodium Diisopropylamide (NDA) Complex and Related Hindered Amides. *J. Organomet. Chem.* **1996**, *518*, 85.

(10) Frisch, M. J.; Trucks, G. W.; Schlegel, H. B.; Scuseria, G. E.; Robb, M. A.; Cheeseman, J. R.; Zakrzewski, V. G.; Montgomery, J. A., Jr.; Stratmann, R. E.; Burant, J. C.; Dapprich, S.; Millam, J. M.; Daniels, A. D.; Kudin, K. N.; Strain, M. C.; Farkas, O.; Tomasi, J.; Barone, V.; Cossi, M.; Cammi, R.; Mennucci, B.; Pomelli, C.; Adamo,

DOI: 10.1021/acs.joc.9b00968
J. Org. Chem. 2019, 84, 9051−9057

C.; Clifford, S.; Ochterski, J.; Petersson, G. A.; Ayala, P. Y.; Cui, Q.; Morokuma, K.; Malick, D. K.; Rabuck, A. D.; Raghavachari, K.; Foresman, J. B.; Cioslowski, J.; Ortiz, J. V.; Baboul, A. G.; Stefanov, B. B.; Liu, G.; Liashenko, A.; Piskorz, P.; Komaromi, I.; Gomperts, R.; Martin, R. L.; Fox, D. J.; Keith, T.; Al-Laham, M. A.; Peng, C. Y.; Gill, A.; Nanayakkara, C.; Gonzalez, M.; Challacombe, P. M. W.; Johnson, B.; Chen, W.; Wong, M. W.; Andres, J. L.; Gonzalez, C.; Head-Gordon, M.; Replogle, E. S.; Pople, J. A. *Gaussian Version 3.09*, revision A.1; Gaussian, Inc.: Wallingford, CT, 2009.

(11) Zhao, Y.; Truhlar, D. G. The M06 Suite of Density Functionals for Main Group Thermochemistry, Thermochemical Kinetics, Noncovalent Interactions, Excited States, and Transition Elements: Two New Functionals and Systematic Testing of Four M06-Class Functionals and 12 Other Functionals. *Theor. Chem. Acc.* **2008**, *120*, 215. We generally avoid overinterpreting the computations quantitatively, instead choosing to use mitigated language such as "computationally viable". We find computations of organosodiums more capricious, occasionally causing failures to converge during MP2 single-point calculations. Although larger basis sets did not solve the problems, Minnesota functionals (M06-2X) precluded the failures and are reputed to be thermochemically superior for main group elements.

(12) (a) Rein, A. J.; Donahue, S. M.; Pavlosky, M. A. In Situ FTIR Reaction Analysis of Pharmaceutical-Related Chemistry and Processes. *Curr. Opin. Drug Discovery Dev.* **2000**, *3*, 734. (b) Defernez, M.; Wilson, R. H. Infrared Spectroscopy: Instrumental Factors Affecting the Long-Term Validity of Chemometric Models. *Anal. Chem.* **1997**, *69*, 1288. (c) Brodmann, T.; Koos, P.; Metzger, A.; Knochel, P.; Ley, S. V. Continuous Preparation of Arylmagnesium Reagents in Flow with Inline IR Monitoring. *Org. Process Res. Dev.* **2012**, *16*, 1102. (d) Connolly, T. J.; Hansen, E. C.; MacEwan, M. F. In Situ FTIR Study and Scale-Up of an Enolization-Azidation Sequence. *Org. Process Res. Dev.* **2010**, *14*, 466.

(13) (a) Günther, H. Selected Topics from Recent NMR Studies of Organolithium Compounds. *J. Braz. Chem. Soc.* **1999**, *10*, 241. (b) Reich, H. J. Role of Organolithium Aggregates and Mixed Aggregates in Organolithium Mechanisms. *Chem. Rev.* **2013**, *113*, 7130.

(14) Tomasevich, L.; Collum, D. B. Method of Continuous Variation: Characterization of Alkali Metal Enolates Using ^{1}H and ^{19}F NMR Spectroscopies. *J. Am. Chem. Soc.* **2014**, *136*, 9710.

(15) IR spectra were simulated using DFT from structures optimized using a relatively high basis set, 6−311+G(2d,p). Starting carbamate **1e** provides a benchmark with a calculated carbamate carbonyl of 1759 cm^{-1} (1728 cm^{-1} observed). The calculated values for disolvated (chelated) monomer **6** (1673 cm^{-1}), trisolvated (chelated) monomer **7** (1682 cm^{-1}), and tetrasolvated (unchelated) monomer **8**(1721 cm^{-1}), when compared with the observed value of the arylsodium **2e** (1673 cm^{-1}), suggest that chelation remains intact.

(16) Nic, M.; Jirat, J.; Kosata, B. An isodesmic reaction is "a reaction (actual or hypothetical) in which the types of bonds that are made in forming the products are the same as those which are broken in the reactants". In *IUPAC. Compendium of Chemical Terminology*, 2nd ed.; McNaught, A. D.; Wilkinson, A., Eds.; Blackwell Scientific Publications: Oxford, 1997; http://goldbook.iupac.org, 0-9678550-9-8.

(17) Low, C. M. R. Product Class 2: Alkyl Aryl ethers—Synthesis by Substitution. *Science of Synthesis* **2007**, *31a*, 547.

(18) The computations use the Gaussian standard state of 1.0 atm. If the THF concentration is corrected to neat THF (approximately 13 M), each solvation step benefits from approximately 2.0 kcal/mol of additional stabilization at −78 °C (195 K). Pratt, L. M.; Merry, S.; Nguyen, S. C.; Quan, P.; Thanh, B. T. A Computational Study of Halomethyllithium Carbenoid Mixed Aggregates with Lithium Halides and Lithium Methoxide. *Tetrahedron* **2006**, *62*, 10821.

(19) Mixtures of arylsodiums of type **2** and phenolates of type **3** do not appear to form mixed aggregates with NaDA. Organosodium mixed and hetero aggregates have been reported previously.[20]

(20) (a) Ojeda-Amador, A. I.; Martinez-Martinez, A. J.; Kennedy, A. R.; O'Hara, C. T. Synthetic and Structural Studies of Mixed Sodium *Bis*(trimethylsilyl)amide/Sodium Halide Aggregates in the Presence of η^2-*N,N*-, η^3-*N,N,N/N,O,N*-, and η^4-*N,N,N,N*-Donor Ligands. *Inorg. Chem.* **2015**, *54*, 9833. (b) For a NaHMDS-sodium enolate mixed aggregate characterized crystallographically, see: Williard, P. G.; Hintze, M. J. Mixed Aggregates: Crystal Structures of a Lithium Ketone Enolate/Lithium Amide and of a Sodium Ester Enolate/Sodium Amide. *J. Am. Chem. Soc.* **1990**, *112*, 8602. (c) Kissling, R. M.; Gagne, M. R. Structure and Reactivity of Mixed Alkali Metal Alkoxide/Aryloxide Catalysts. *J. Org. Chem.* **2001**, *66*, 9005.

(21) (a) Algera, R. F.; Gupta, L.; Hoepker, A. C.; Liang, J.; Ma, Y.; Singh, K. J.; Collum, D. B. Lithium Diisopropylamide: Non-Equilibrium Kinetics and Lessons Learned about Rate Limitation. *J. Org. Chem.* **2017**, *82*, 4513. (b) Bissette, A. J.; Fletcher, S. P. Mechanisms of Autocatalysis. *Angew. Chem., Int. Ed.* **2013**, *52*, 12800.

(22) We define the idealized rate law as that obtained by rounding the observed reaction orders to the nearest rational order.

(23) Edwards, J. O.; Greene, E. F.; Ross, J. From Stoichiometry and Rate Law to Mechanism. *J. Chem. Educ.* **1968**, *45*, No. 381. The rate law provides the stoichiometry of the transition structure relative to that of the reactants.

(24) Intrinsic reaction coordinate (IRC) calculations are defined as "the minimum energy reaction pathway (MERP) in mass-weighted cartesian coordinates between the transition state of a reaction and its reactants and products." They show the minima preceding and following transition state.

(25) The preference for the meta adduct **17** is consistent with literature reports and the developing stabilization of the arylsodium by either induction or chelation in the transition state. (a) Candito, D. A.; Dobrovolsky, D.; Lautens, M. Development of an Intramolecular Aryne Ene Reaction and Application to the Formal Synthesis of (±)-Crinine. *J. Am. Chem. Soc.* **2012**, *134*, 15572. (b) Hickey, M. R.; Allwein, S. P.; Nelson, T. D.; Kress, M. H.; Sudah, O. S.; Moment, A. J.; Rodgers, S. D.; Kaba, M.; Fernandez, P. Process Development and Pilot Plant Synthesis of Methyl 2-Bromo-6-chlorobenzoate. *Org. Process Res. Dev.* **2005**, *9*, 764.

(26) (a) Ramírez, A.; Candler, J.; Bashore, C. G.; Wirtz, M. C.; Coe, J. W.; Collum, D. B. Formation of Benzynes from 2,6-Dihaloaryllithiums: Mechanistic Basis of the Regioselectivity. *J. Am. Chem. Soc.* **2004**, *126*, 14700. (b) Riggs, J. C.; Ramírez, A.; Cremeens, M. E.; Bashore, C. G.; Candler, J.; Wirtz, M. C.; Coe, J. W.; Collum, D. B. Structural and Rate Studies of the Formation of Substituted Benzynes. *J. Am. Chem. Soc.* **2008**, *130*, 3406.

DOI: 10.1021/acs.joc.9b00968
J. Org. Chem. 2019, 84, 9051−9057